

A satellite image of the Pacific Ocean, showing the western coast of North America on the left and the eastern coast of South America on the right. The ocean surface is covered with a complex pattern of white and light blue lines, representing internal gravity waves. These waves are most prominent in the central and eastern parts of the image, showing a series of parallel, wavy lines that stretch across the ocean. The background is a deep blue color.

Oceanic Balanced Motions and Internal Gravity Waves from Space: using LLC4320

Hector S. Torres, Zhan Su
Caltech/JPL, Pasadena, CA

Collaborators:

^{1,2}Patrice Klein, ¹Andrew Thompson, ¹Dimitris Menemenlis, ¹Jinbo Wang, ³Christopher Henze, ¹Lee-Lueng Fu

¹Jet Propulsion Laboratory/Caltech, ²LOPS-IFREMER/CNRS France, ³NASA AMES Center



Jet Propulsion Laboratory
California Institute of Technology

Balanced motions: Meso/sub-mesoscale motions

Mesoscale balanced motions:

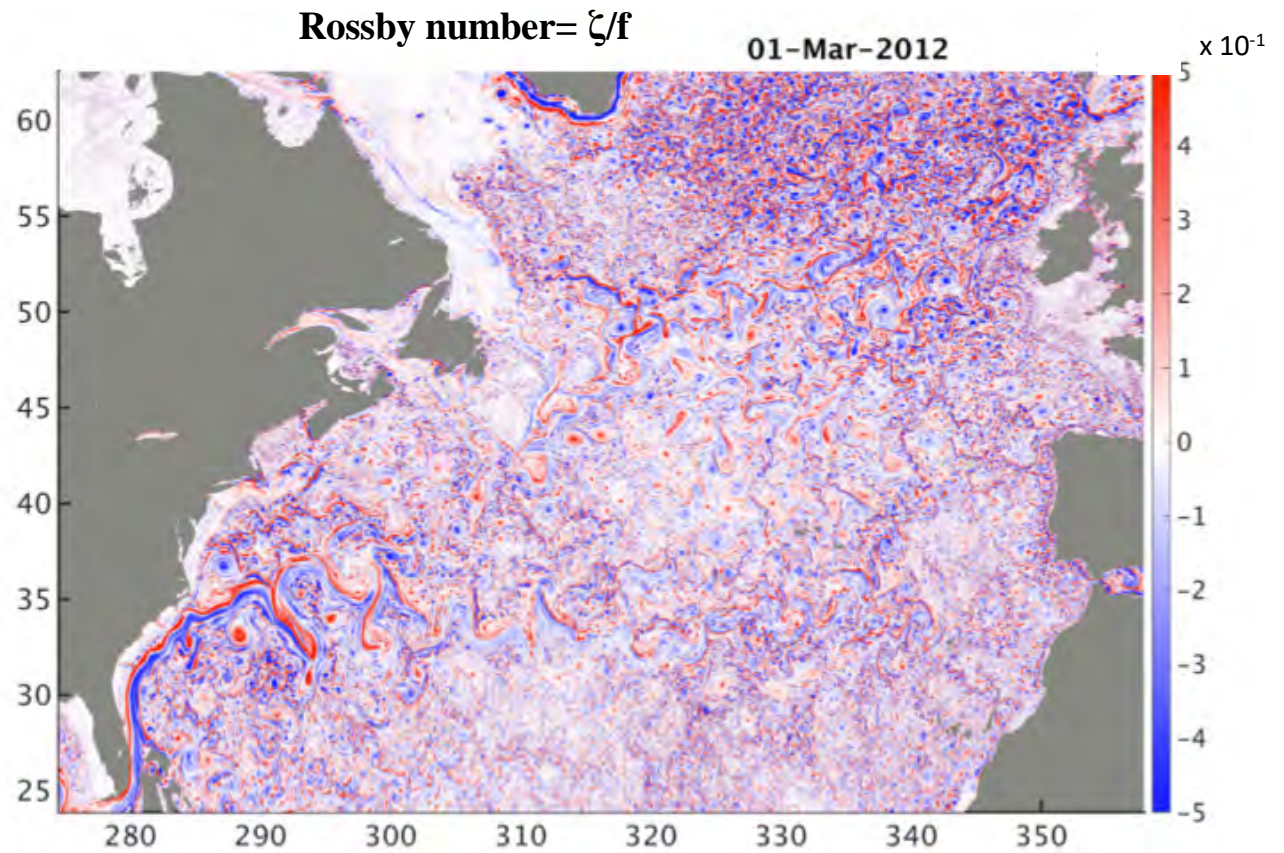
- Mesoscale eddies (50 – 200 km)
- Impact on **horizontal** fluxes of heat and momentum

Submesoscale balanced motions:

- Frontal structures and smaller eddies (1 – 50 km)
- Impact on **vertical** fluxes of heat and momentum

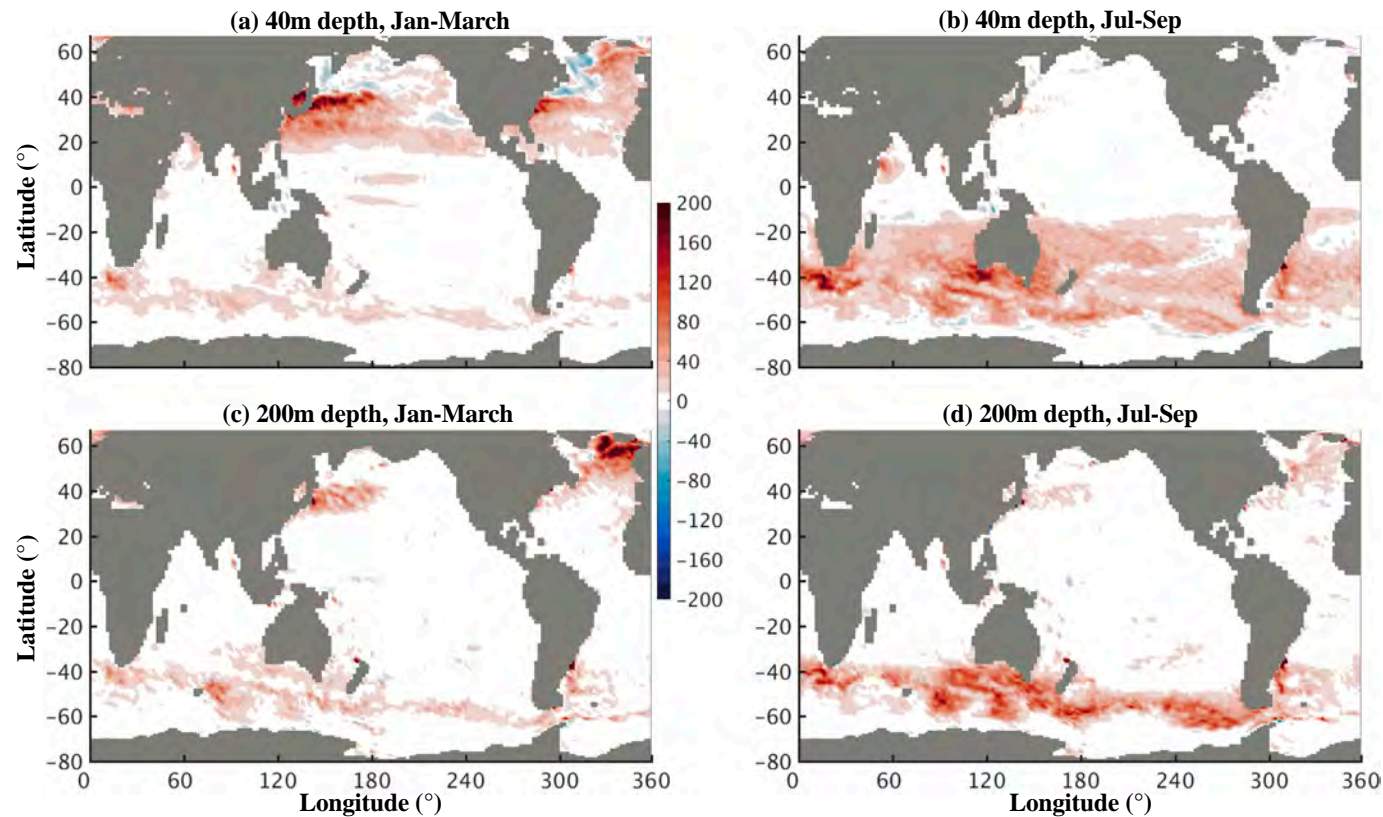
Submesoscale motions (1–50 km) have strong vertical velocities lead to vertical exchanges between the upper and interior ocean

Where and when?



LLC4320 simulation

Submesoscale motions lead to upward vertical heat fluxes, up to 100 W/m^2
--> air-sea interactions

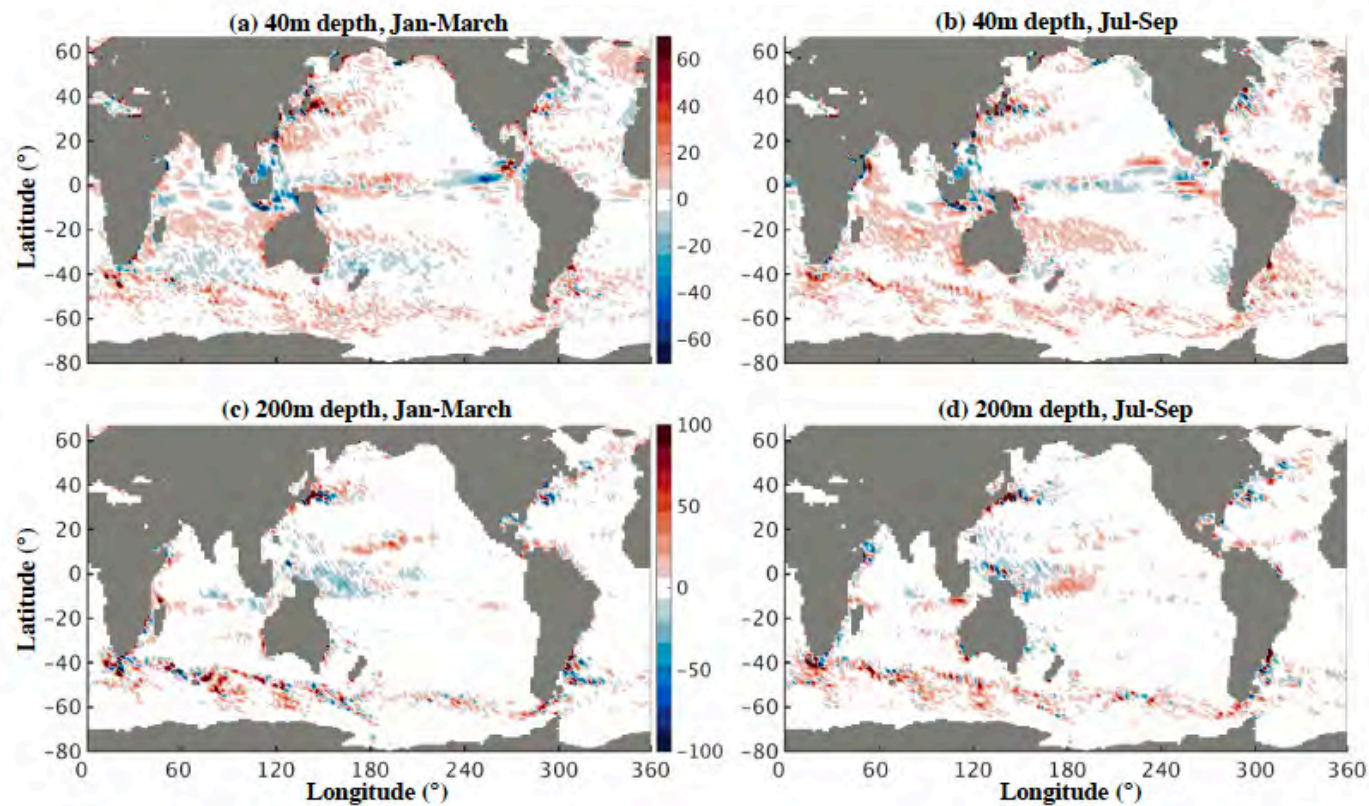


Up-gradient vertical heat
fluxes and not down-
gradient vertical heat
fluxes

Global maps of the vertical heat fluxes in the **submesoscale band [10 – 50 km]** (W/m^2). **20-100 W/m^2 .**

Su et al. 2017,
Nature communications,
under review

Mesoscale eddies have a weak impact on the vertical heat fluxes



3 times smaller than the submesoscale part!

Global maps of the vertical heat fluxes in the mesoscale band [50 – 100 km] (W/m^2).

Submesoscale permitting and tidal-resolving simulation

Balanced motions (BMs):
Slow motions: $\omega < f$

Internal gravity waves (IGWs):
Fast motions: $\omega > f$

From the Hyperwall (Chris Henze)

-88.175 m)

Southern Ocean

il 2012 05:00

How to discriminate BMs from IGWs: frequency-wavenumber spectrum

- Frequency-wavenumber spectrum (numerical simulations):

Continuity for BMs

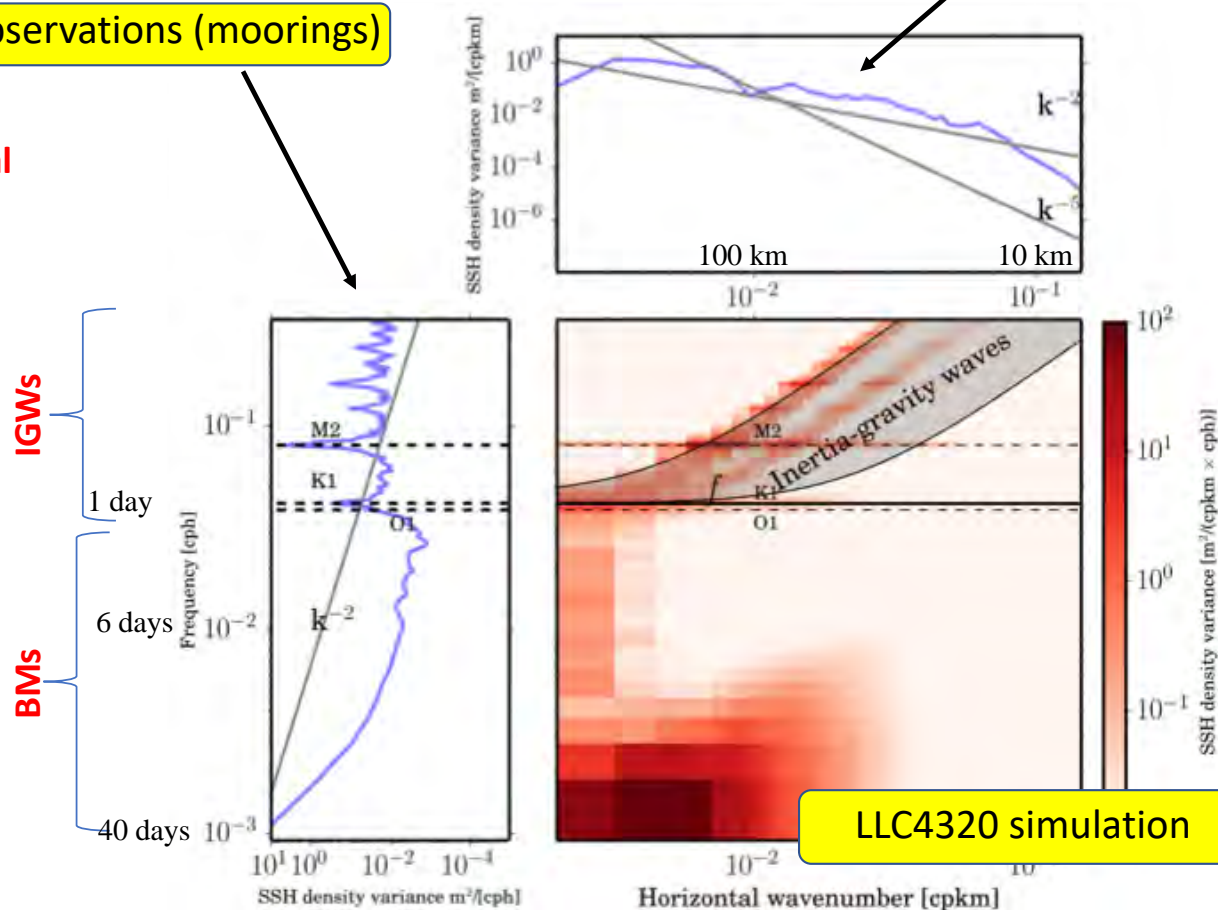
- Indicating strong nonlinear interactions

Dispersion relation curves following **discrete beams for IGWs**

- Indicating weak nonlinear interactions

In-situ observations (moorings)

Space observations



Need to monitor these two classes of motions in the global ocean because of their different impacts on the energy budget

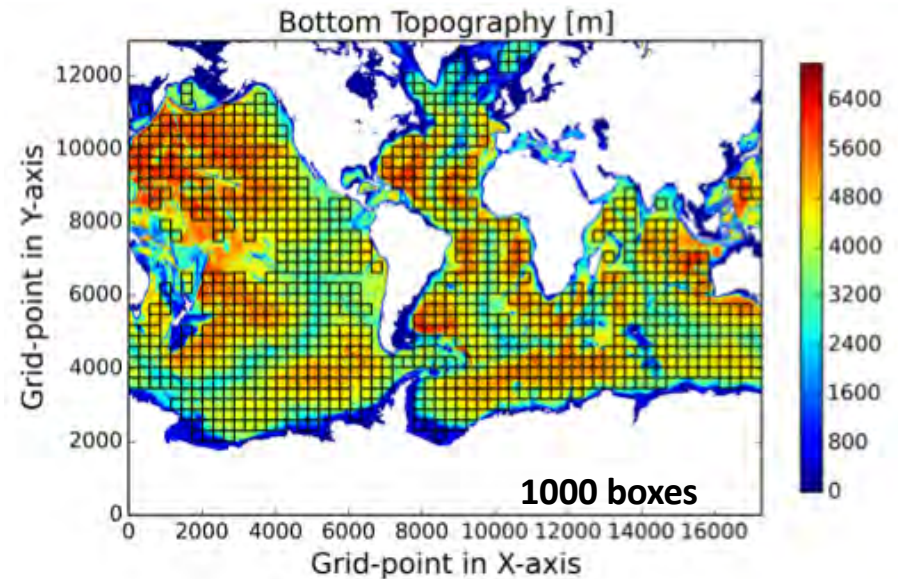
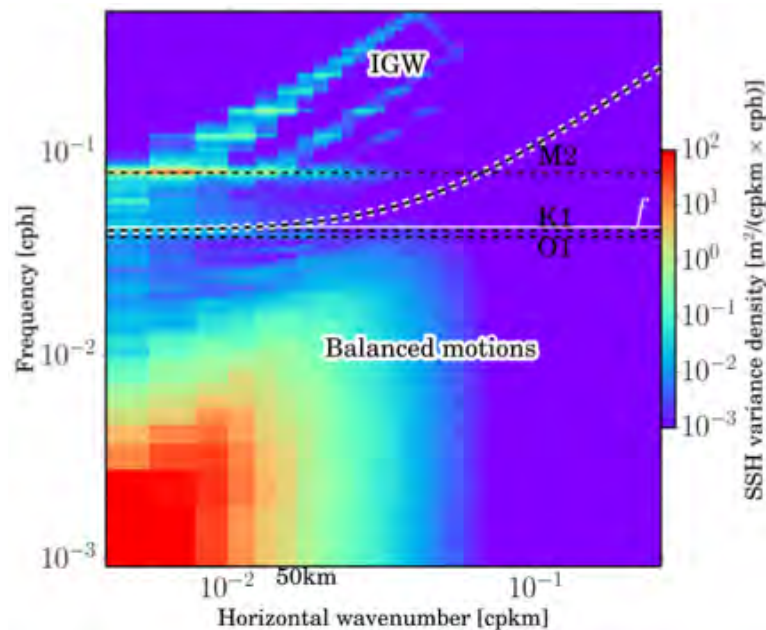
Our project is to better understand the respective signature of BMs and IGWs on the different oceanic fields observable from space: SSH, KE, SST, SSS

How to discriminate these two classes of motions in high-resolution observations?

Using frequency-wavenumber spectrum to partition IGWs and BMs

We can define the ratio, R , between the variance associated with BMs and that associated with IGWs (using the dispersion relation curve for the highest baroclinic mode to partition the two classes of motion)

$$R = BMs/IGWs$$



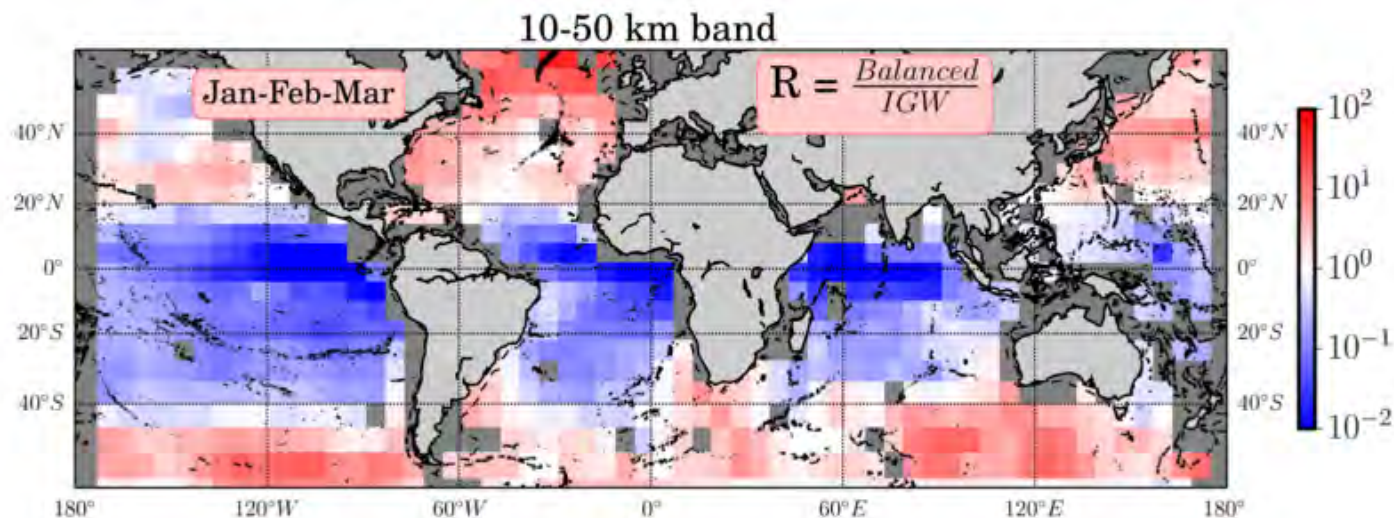
This has been done for SSH, KE, relative vorticity (RV), divergence (DIV), SST, and sea surface salinity (SSS)

Two scale ranges are considered:

- 10 – 50 km (from Su et al. 2017)
- 50 – 100 km

12,000 frequency-wavenumber spectra computed

Global maps of R value, $R = \frac{BM_s}{IGW_s}$, example



For a given spatial-scale
band and a given variable

**$R > 1$ means that the variability of
the flow is explained by BMs**

$R = 1$ means that is difficult to
distinguish

**$R < 1$ means that the variability of
the flow is explained by IGWs**

Differences between Northern and Southern Hemispheres: Northern Hemisphere more affected by IGWs in the 10—50km band

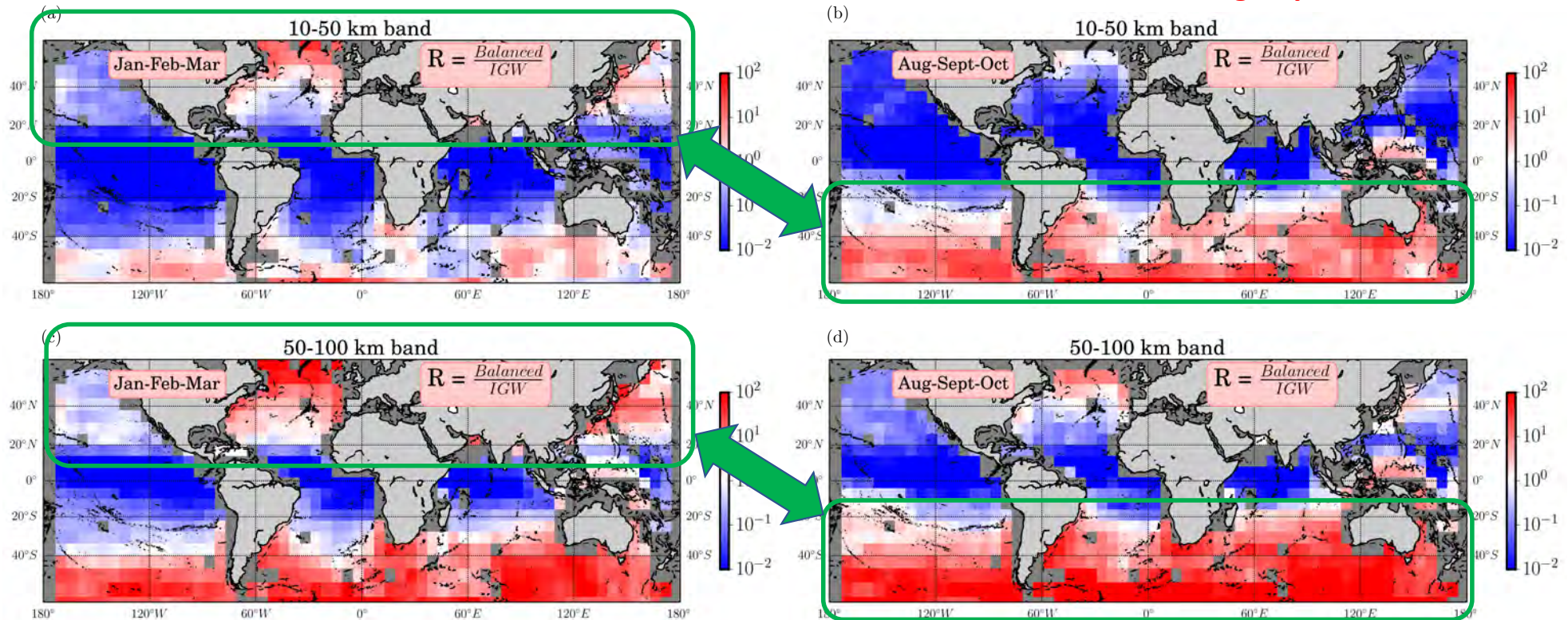
Jan-Feb-Mar

Global maps of R values for SSH

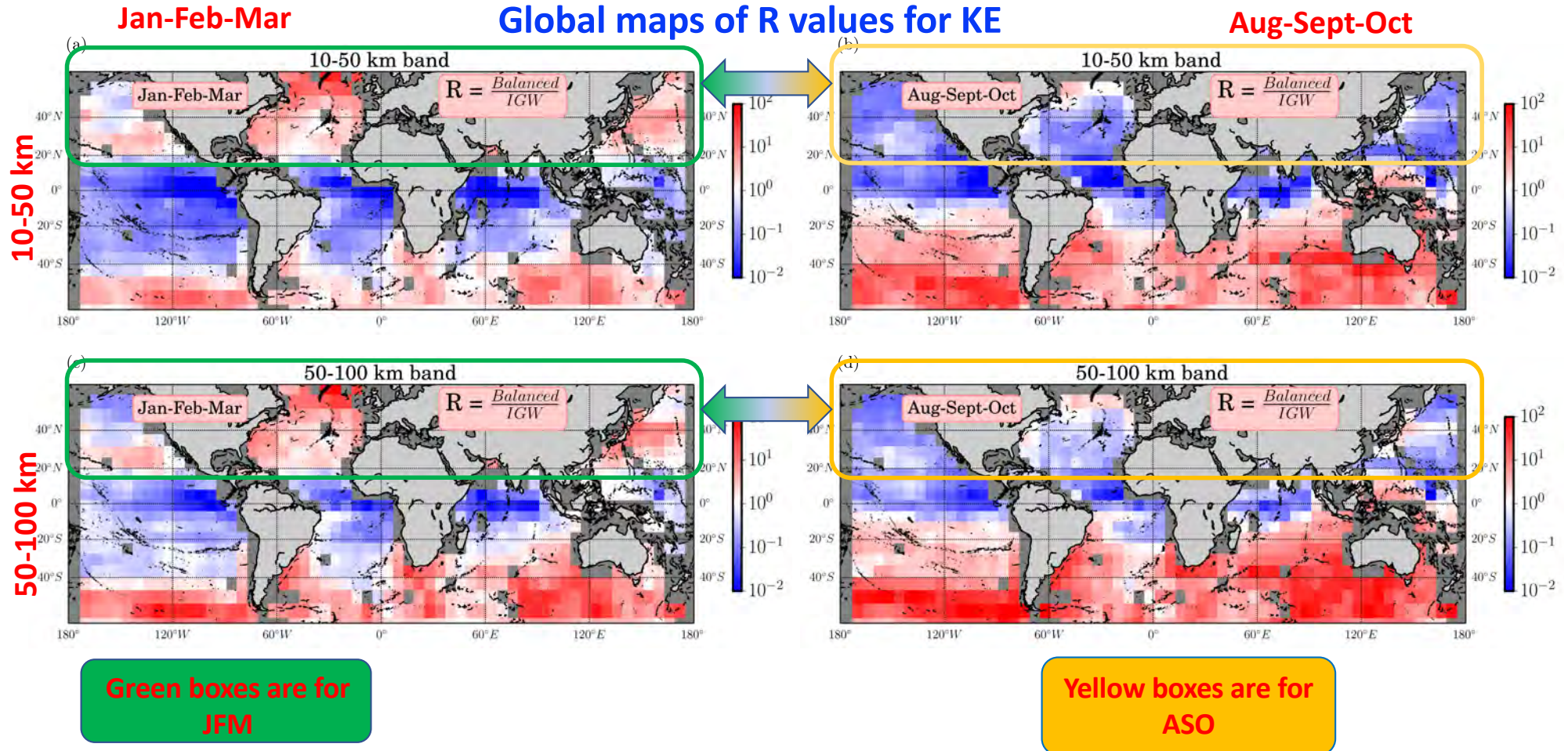
Aug-Sept-Oct

10-50 km

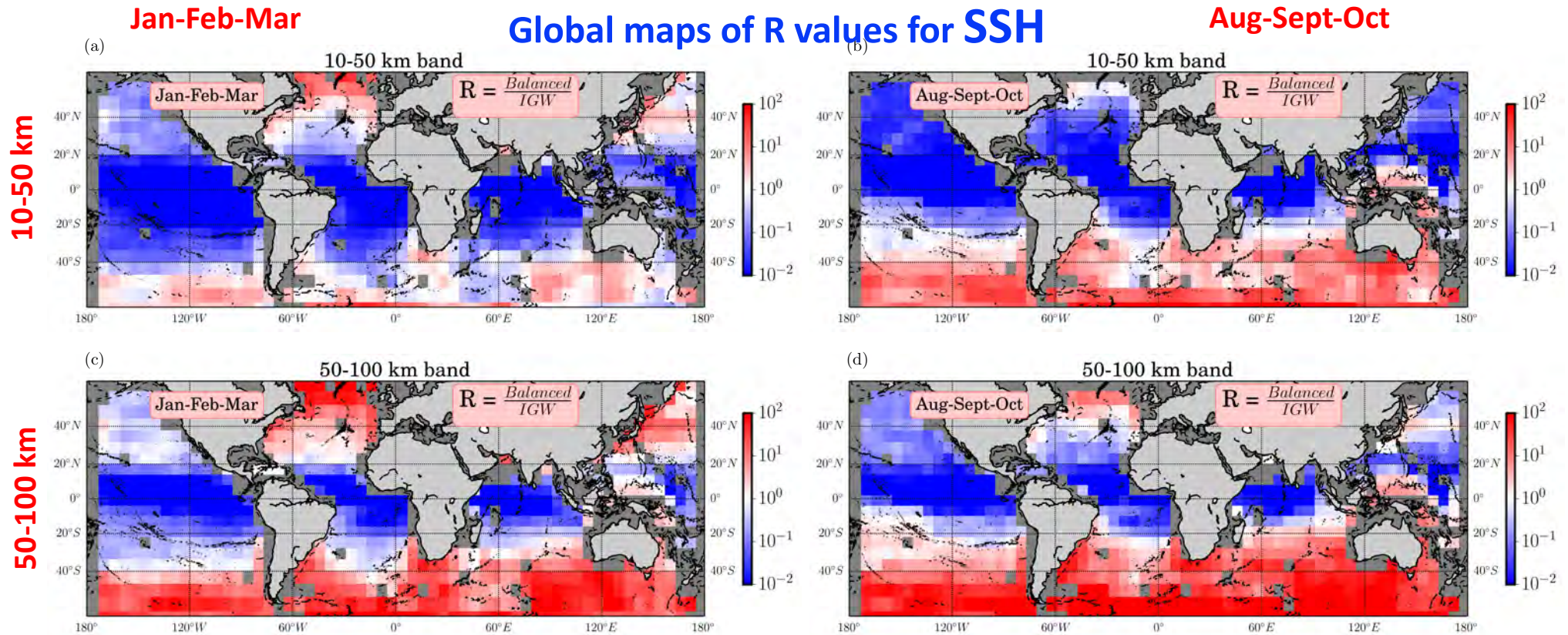
50-100 km



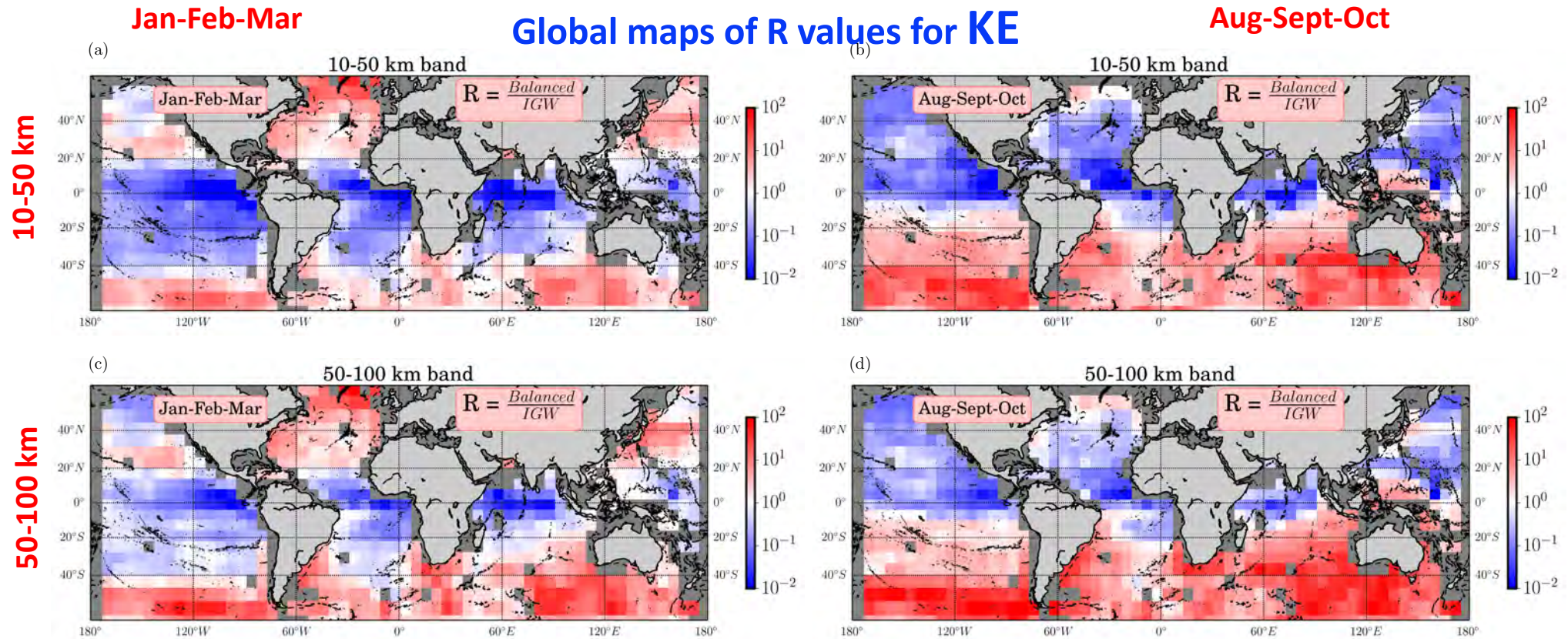
Differences between summer and winter: Strong seasonality in each Hemisphere, with IGWs more dominant in summer and BMs in winter



Differences between SSH and KE: IGWs have impact on both fields with larger contrast for SSH



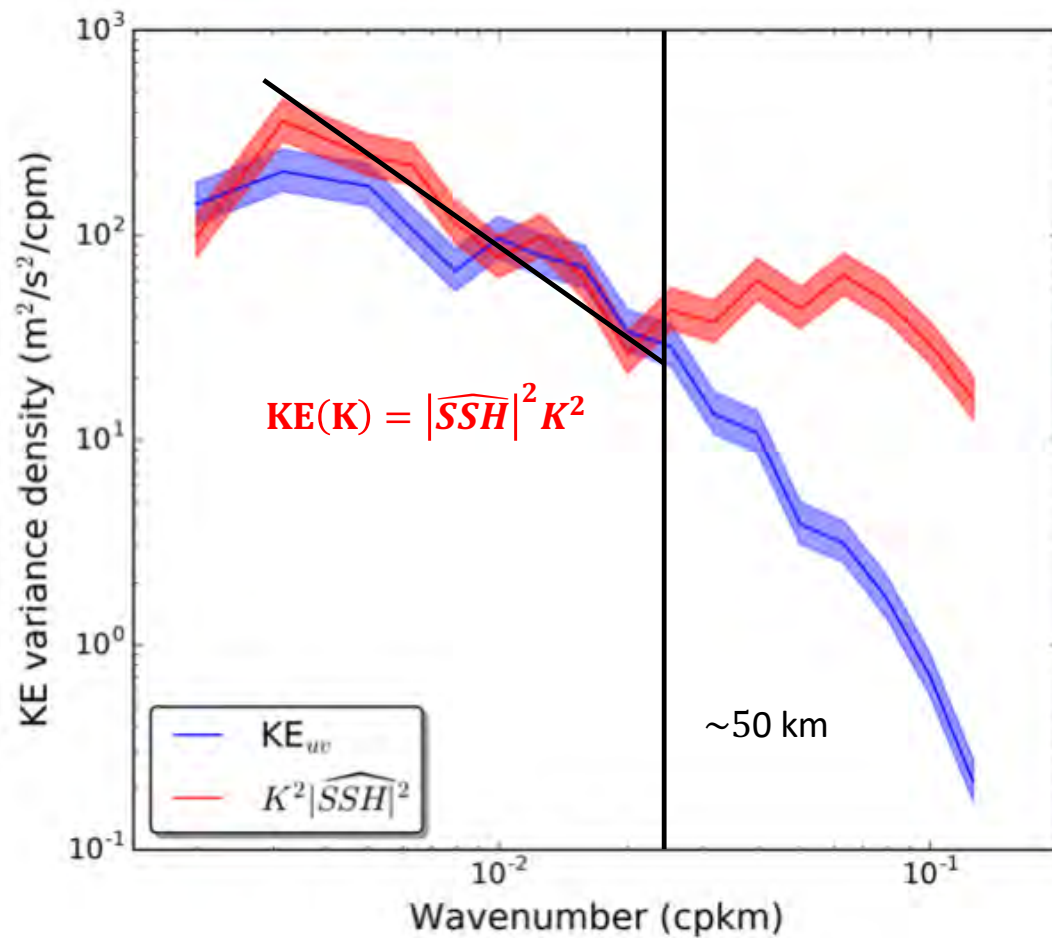
Differences between SSH and KE: IGWs have impact on both fields with larger contrast for SSH



KE spectra deduced from surface motions and that deduced from SSH

For BMs (> 50 km), the relation between Potential Energy (PE) and Kinetic Energy (KE) in spectral space is (assuming geostrophic balance and isotropy)

$$KE(K) = |\widehat{SSH}|^2 K^2$$



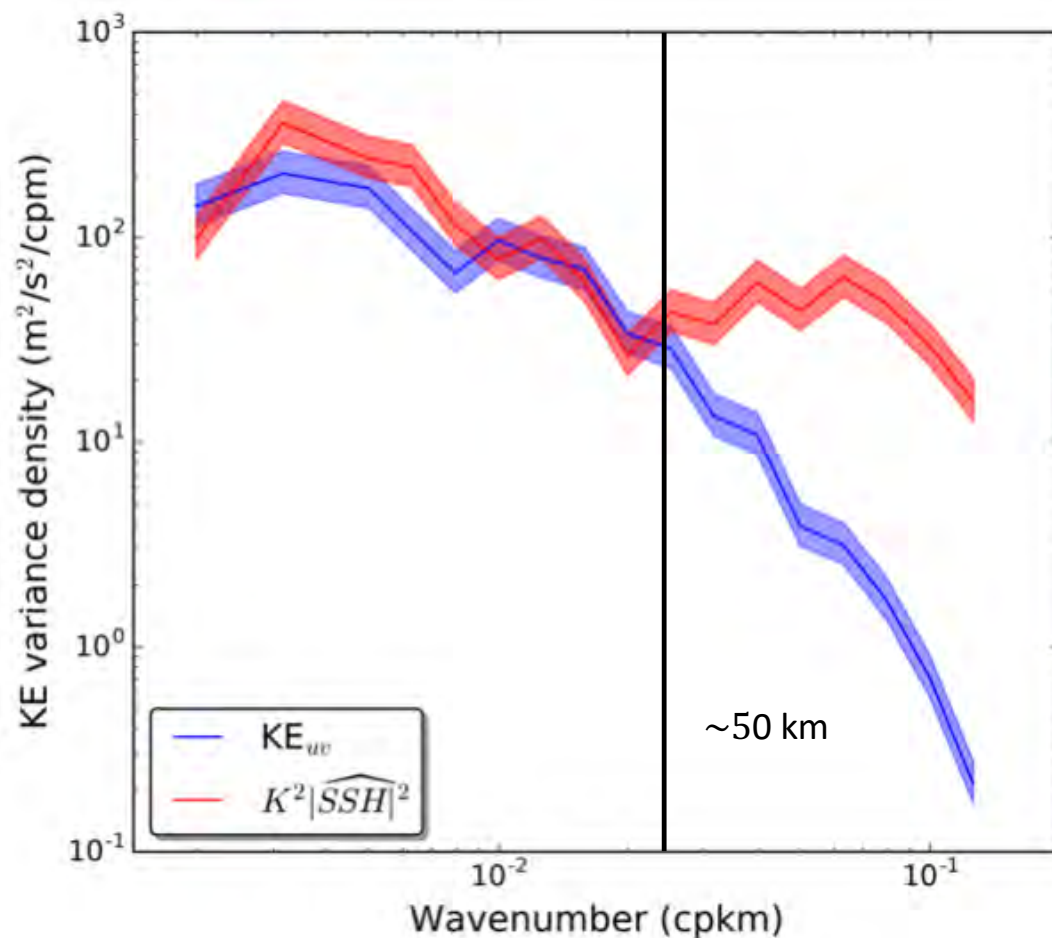
Region: California Current
Season: summer

KE spectra deduced from surface motions and that deduced from SSH

- For scales smaller than 50 km, the spectral slope for $K^2 |\widehat{SSH}|^2$ becoming much shallower

If KE departs from this relation, it means a loss of balance

=> This discontinuity of the SSH spectral slope is not observed in HR simulations without tides (Chassignet and Xu, JPO 2017)



Region: California Current
Season: summer

KE spectra deduced from surface motions and that deduced from SSH

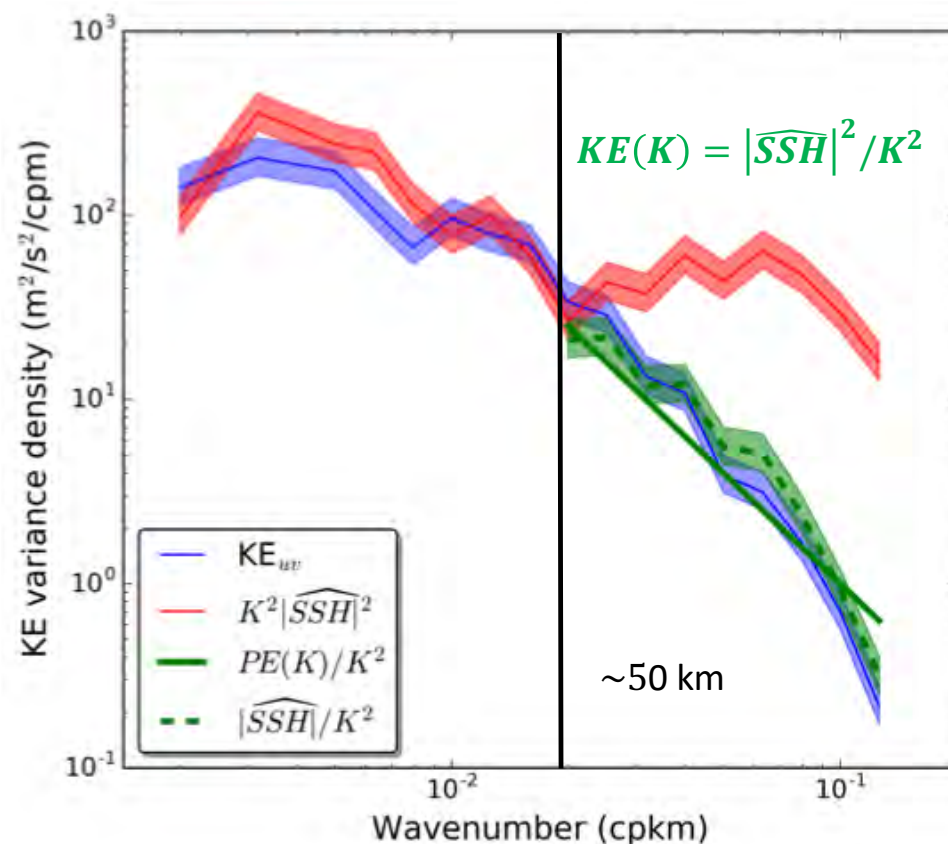
For BMs (< 50 km), ~~$KE(K) = |\widehat{SSH}|^2 K^2$~~

Based on the linearized shallow water model (Gill, 1982),

$$KE(K) = |\widehat{SSH}|^2 / K^2$$

Here we use SSH like proxy of PE

The significant discontinuity in the PE spectral slope thus characterize the IGW impact on SSH and therefore the loss of balance in this scale band, 10–50 km



Region: California Current
Season: summer

Summary

- I. Differences between Northern and Southern Hemispheres: Northern Hemisphere is more affected by IGWs than Southern Hemisphere, with these discrepancies mostly pronounced during summer for the 10 - 50 km.
- II. Differences between summer and winter: The seasonality concerns all regions but emphasized in the Northern Hemisphere. Its strongest amplitude is observed in low EKE regions, mostly in the 10 - 50 km.
- III. Differences between SSH and KE: Regions of the KE field where $R \leq 1$, the SSH field often displays even much smaller values ($R \ll 1$). In the Northern Hemisphere, such differences are mostly in the 10-50 km band.
- IV. Impact of BMs and IGWs on SST and SSS: SST and SSS in the 10 - 100 km band are not affected at all by IGWs.

Need to monitor these two classes of motions in the global ocean because of their different impacts on the energy budget

Image credit: NASA

One way to address this need is exploiting the synergy of existing and future satellite observations

- Conventional altimetry (existing JASON I-III)
- SWOT (to be launched in 2021)
- DopplerScatt (project in progress)
- SST (MUR)
- Sea surface salinity (SMAP)



Smoke on the water

By

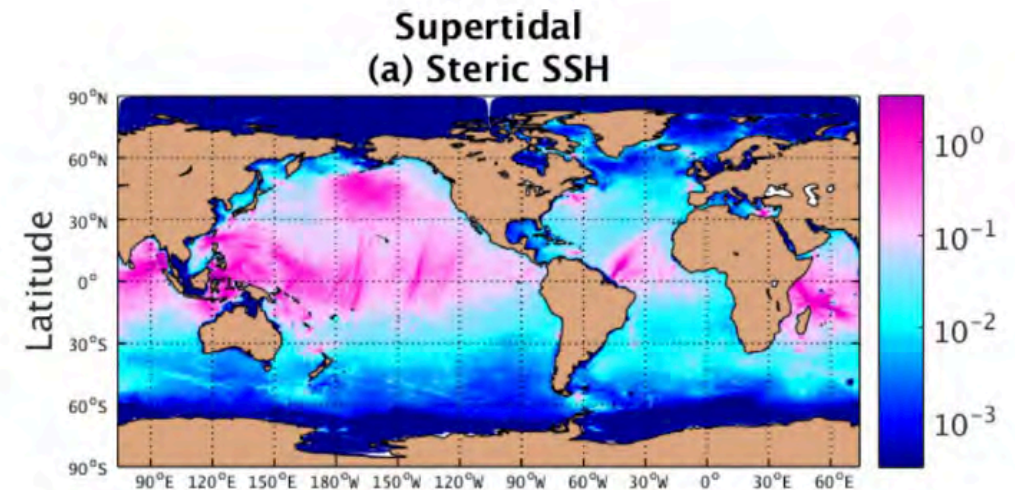
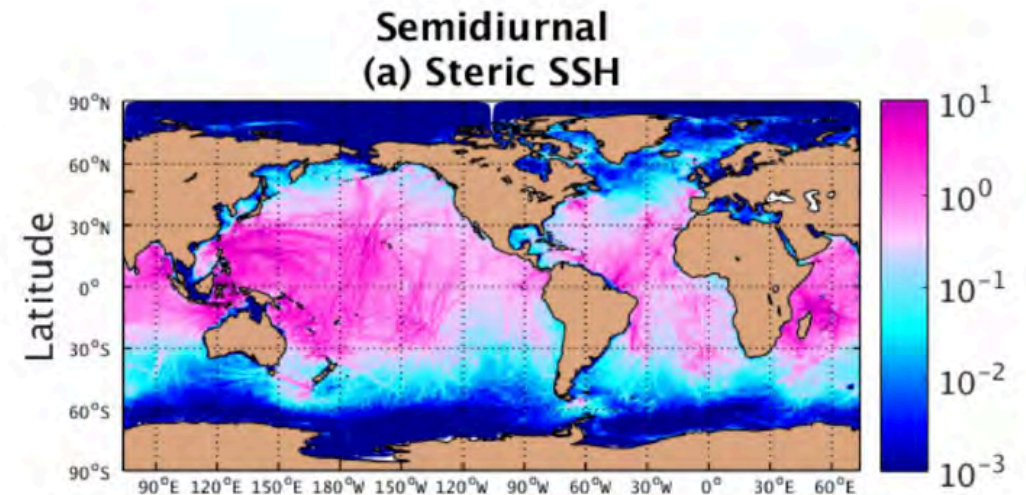
Chris Henze

Thank you,



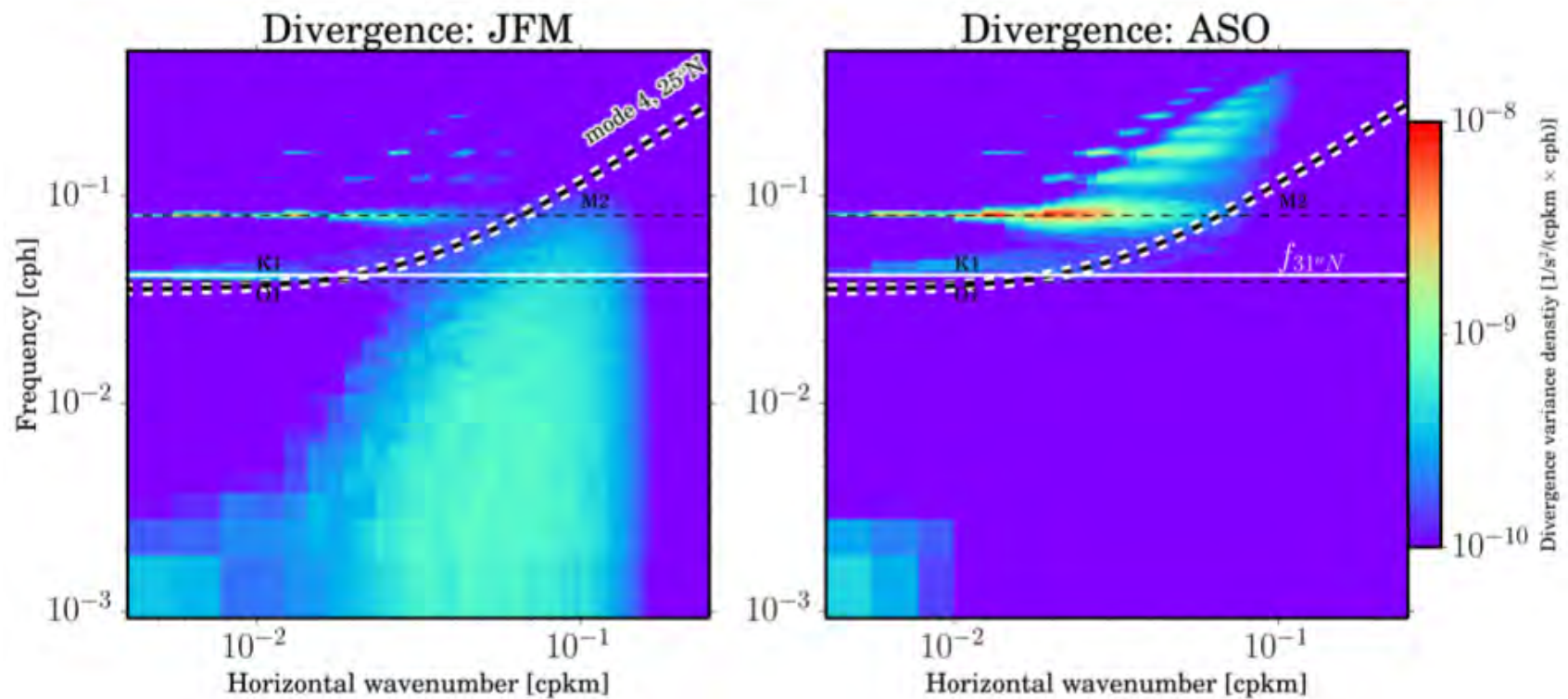
Differences between Northern and Southern Hemispheres

- Energy associated with internal tides (Savage et al. 2017):
 - Mostly energetic in the latitude band between 30° S and 30° N
 - Outside this band internal tides are still energetic in the Northern Hemisphere
 - Also, super-tidal motions are more energetics in the Northern Hemisphere



In the upper oceanic layer: asymmetric seasonal variability of
 BMs and IGWs

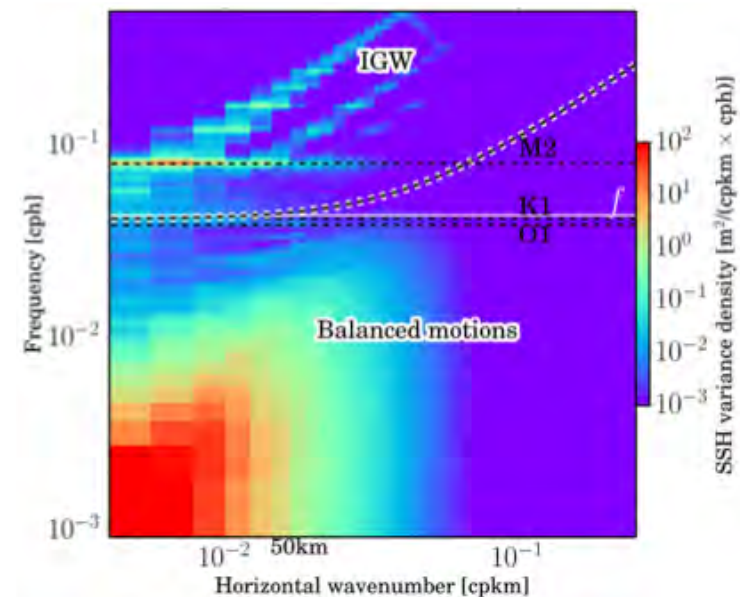
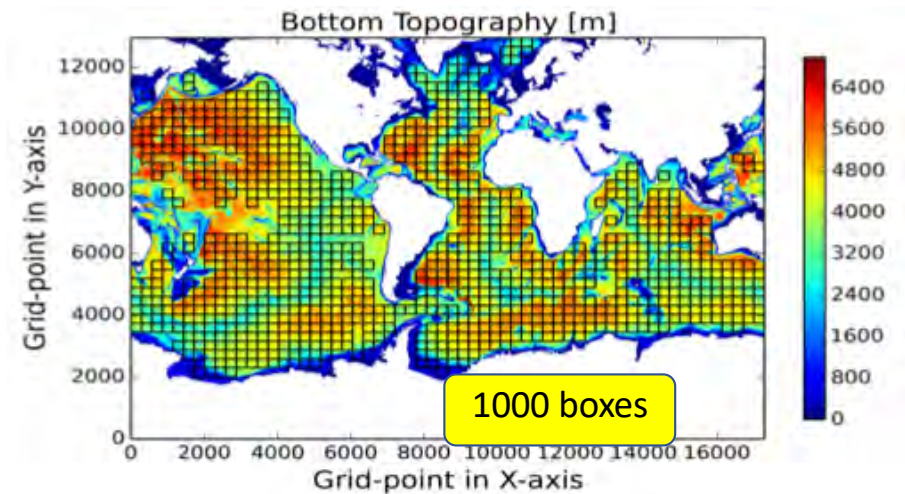
Kuroshio Extension: $6^\circ \times 6^\circ$ box



Frequency-Wavenumber spectrum of divergence, Kuroshio Extension

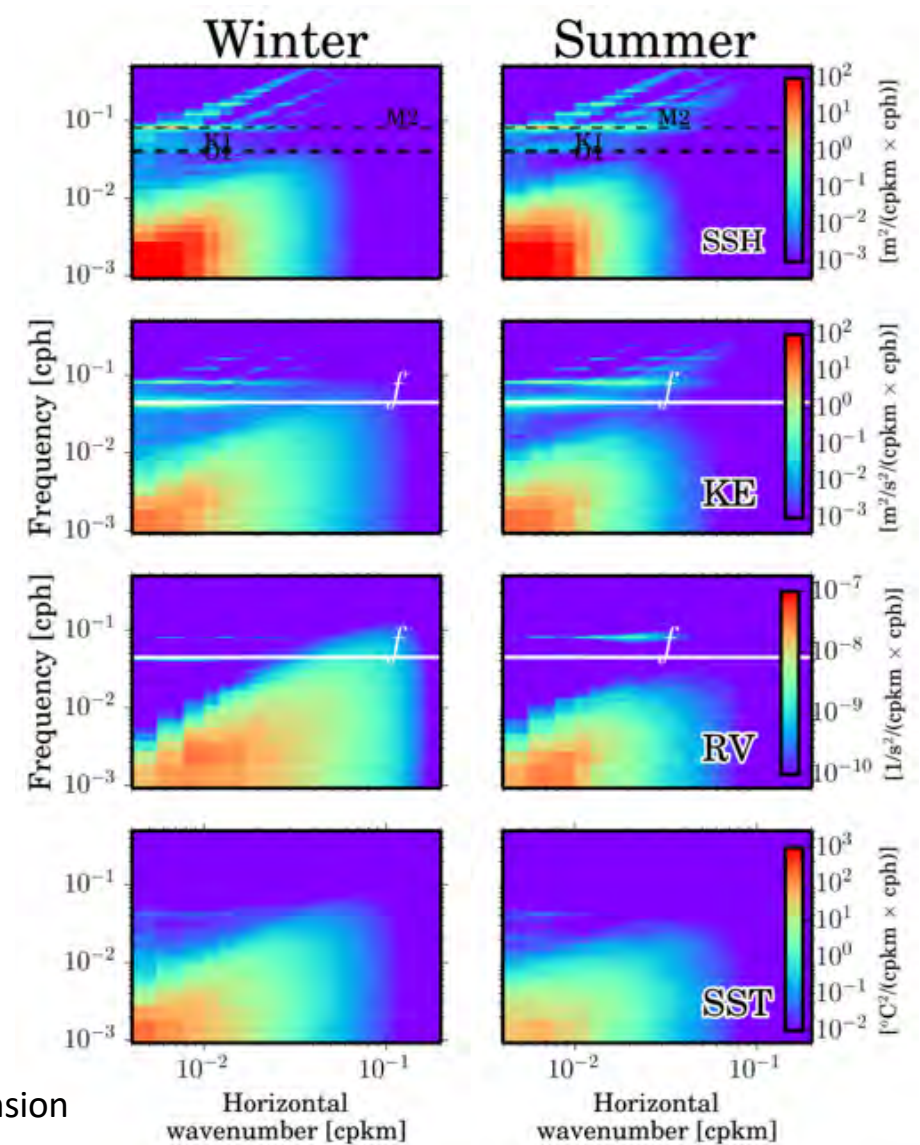
Estimation of **R** in the global ocean: small boxes

- $\sim 6^\circ \times \sim 6^\circ$ grid points
- Temporal coverage: 90 days
- Two seasons:
 - Jan.-Feb.-Mar.
 - Aug.-Sept.-Oct.
- The frequency-wavenumber spectrum was computed for a given variable in each box: (1000 boxes x 2 seasons x 6 variables = **12,000 frequency-wavenumber spectrum**)
- Solving a classical Sturm-Liouville problem produced the n Rossby radii of deformation and therefore the n dispersion relation



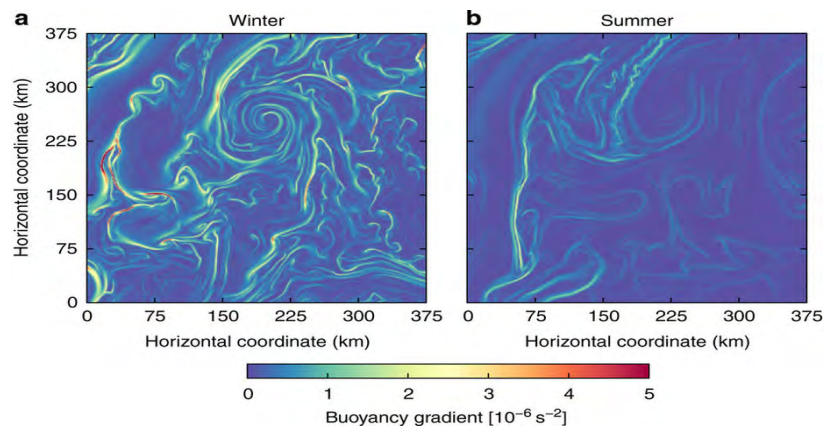
Signature of BMs and IGWs on different oceanic quantities

- Strong impact of IGWs on SSH and KE
- Negligible impacts of IGWs on RV and SST
- BMs more energetic in winter
- Amplification of higher baroclinic modes in summer explain a large part of the IGW seasonality

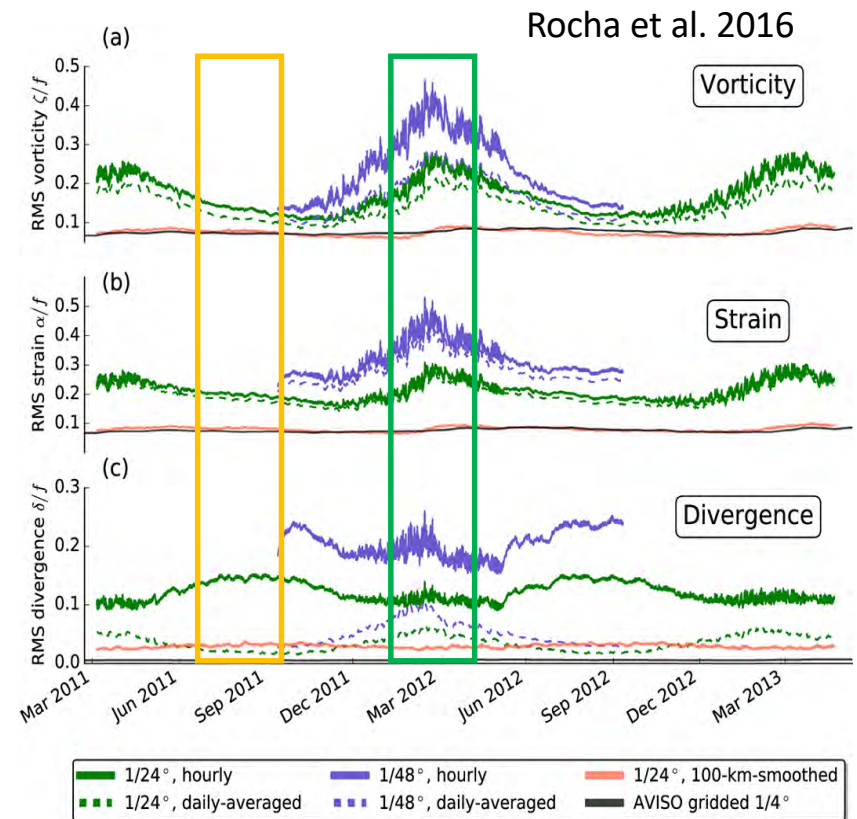


Upper oceanic layer: seasonality of BMs and IGWs

Callies et al. 2015



- **Strong dissymmetric seasonality of BMs and IGWs**
 - **August to October:** IGWs dominate the variance of the flow
 - **January to April:** BMs dominate the variance of the flow



My project:

Before examining how to exploit the synergy of using these different satellite observations, we need to better know the respective signature of BMs and IGWs on the different oceanic fields observable from space

How to discriminate these two classes of motions in high-resolution observations?

Results

- I. Differences between Northern and Southern Hemispheres: Northern Hemisphere is more affected by IGWs than Southern Hemisphere, with these discrepancies mostly pronounced during summer for the 10 - 50 km.
- II. Differences between summer and winter: The seasonality concerns all regions but emphasized in the Northern Hemisphere. Its strongest amplitude is observed in low EKE regions, mostly in the 10 - 50 km.
- III. Differences between SSH and KE: Regions of the KE field where $R \leq 1$, the SSH field often displays even much smaller values ($R \ll 1$). In the Northern Hemisphere, such differences are mostly in the 10-50 km band.
- IV. Impact of BMs and IGWs on SST and SSS: SST and SSS in the 10 - 100 km band are not affected at all by IGWs.



MITgcm model:

The background of the slide is a global map of the world's oceans. The map is color-coded to represent current speeds, with a color bar on the right side ranging from 0.0 to 1.0 m/s. The colors transition from dark blue (0.0) to light blue (0.1-0.2), then to green (0.3-0.4), yellow (0.5-0.6), and finally to orange and red (0.7-1.0). The map shows complex patterns of currents, particularly in the North Atlantic, the Indian Ocean, and the Southern Ocean. The continents are shown in black.

- $1/48^\circ$ global ocean simulation
- **Tides**: 16 harmonics
- 90 vertical levels
- High-frequency atmos. Forcing (ERA-Interim)
- Hourly outputs

Run on Pleiades: NASA supercomputer: **5PFs**
(Sequoia (doe/LLNL): 17PFs; Sunway: 93PFs)

Simulation duration: 13 months (starting from LLC2160 outputs), Sept.2011-Nov.2012

Comparison with in-situ
observations:

Moorings and Gliders data
(Rocha et al. 2016a,b;
Savage et al. 2017a,b,
Drushka et al. 2017;
Viglione et al. 2017; ...)

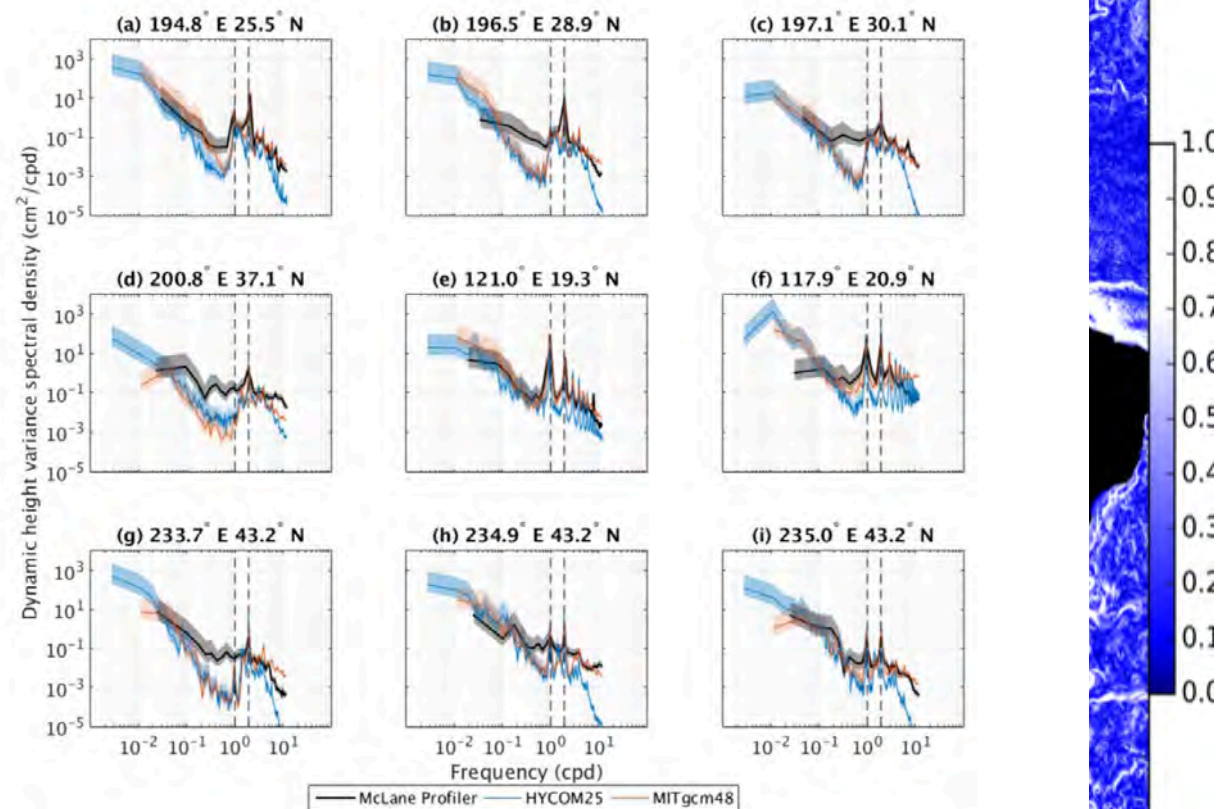


Figure 3. Dynamic height variance frequency spectral densities from McLane profilers and nearest neighbor HYCOM25 and MITgcm48 grid points. The dashed vertical lines denote K_1 diurnal and M_2 semidiurnal tidal frequencies. The shaded regions are the 95% confidence intervals that account only for random error in spectral density calculations.

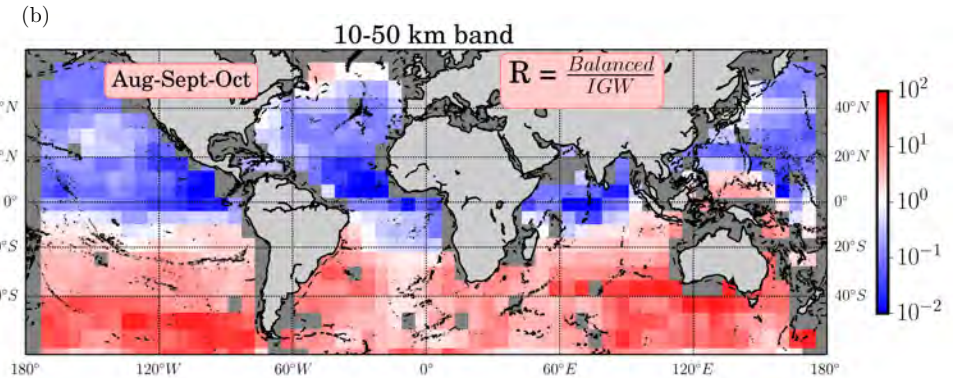
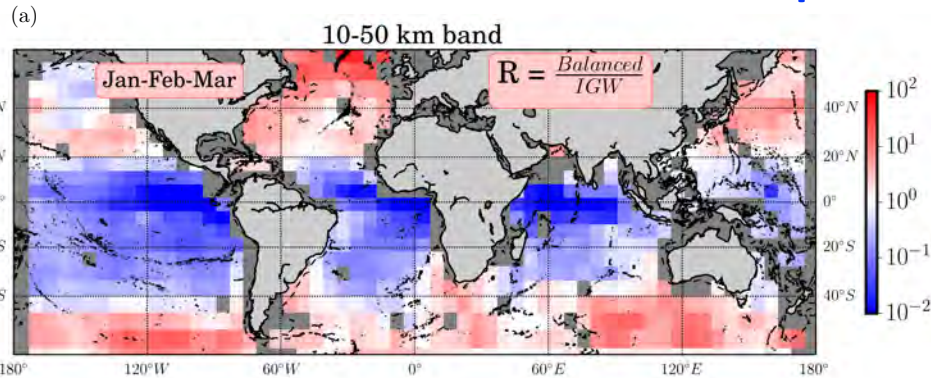
Differences between KE and RV: BM are more dominant in the RV field compare to KE in both Hemispheres, but only for the period Aug-Sept-Oct

Jan-Feb-Mar

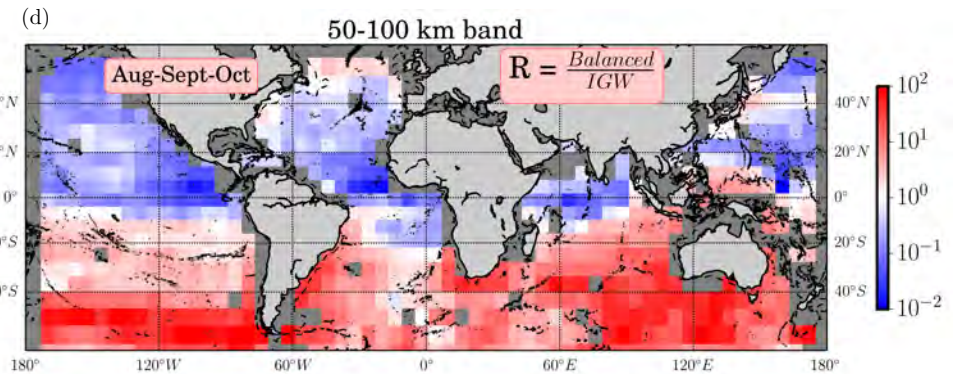
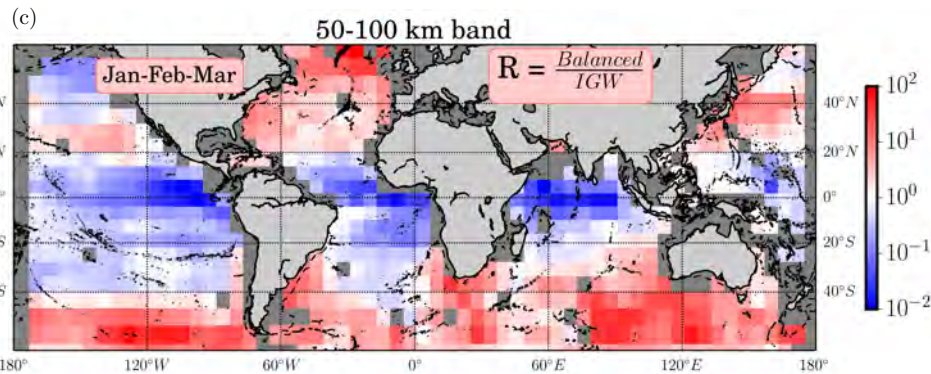
Global maps of R values for KE

Aug-Sept-Oct

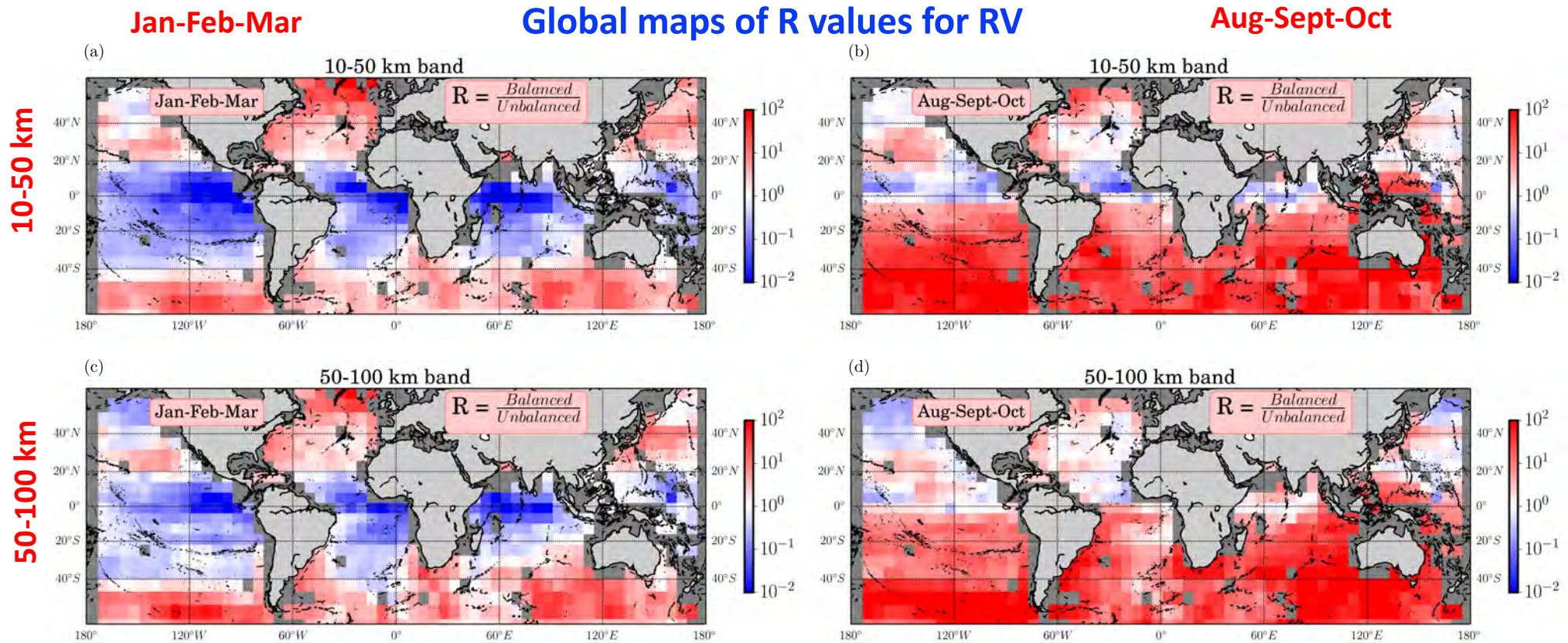
10-50 km



50-100 km



Differences between KE and RV: BM are more dominant in the RV field compare to KE in both Hemispheres, but only for the period of Aug-Sept-Oct



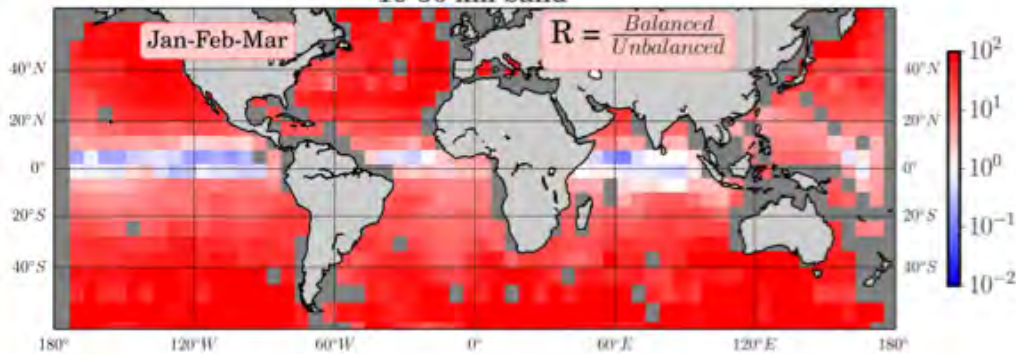
No impact of IGWs on SST and SSS

Global maps of R values for SST

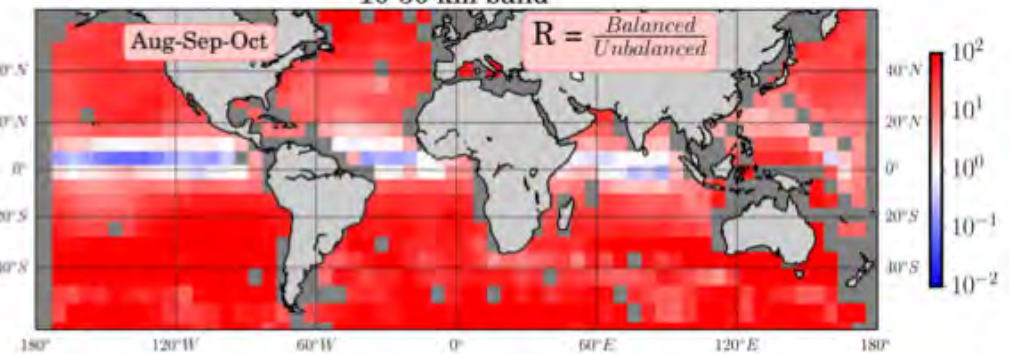
Jan-Feb-Mar

Aug-Sept-Oct

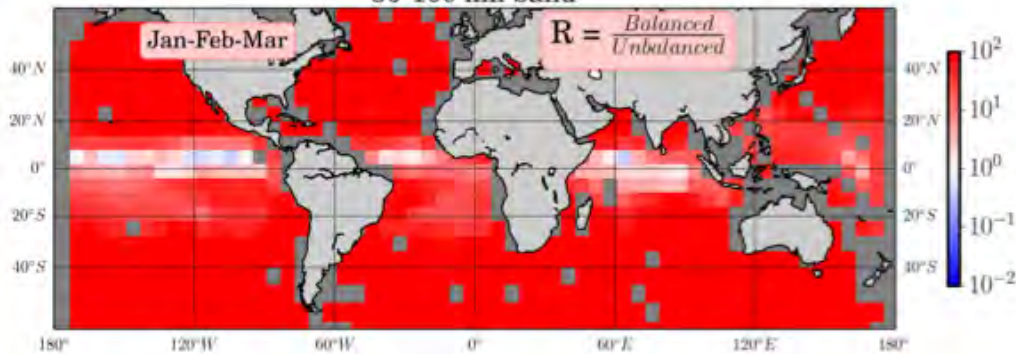
10-50 km band



10-50 km band



50-100 km band



50-100 km band

